Evaluation of chemopreventive potential of xanthone from *Swertia chirata* against DMBA/croton oil-induced chemical carcinogenesis in Swiss mice

Atish Barua, Pritha Choudhury, Chinmay Kumar Panda and Prosenjit Saha*

Chittaranjan National Cancer Institute, Shyama Prasad Mukherjee Road, Bakul Bagan, Bhowanipore, Kolkata 700 026, India

The present study was designed to determine the chemopreventive efficiency of 1,5,8-trihydroxy-3-methoxy xanthone, abbreviated as TMX, isolated and purified from the aerial part of the plant *Swertia chirata* against 9,10-dimethylbenz[a]-anthracene (DMBA)/croton oil-induced skin cancer, and probe into the molecular mechanism. All the mice in the carcinogen control group developed severe dysplastic lesions after the 14th week of application of the carcinogen, which progressed to carcinoma *in situ* around the 20th week; this was validated histologically. However, after TMX treatment, only around 50% of mice developed papilloma which histologically was found to be restrictive to moderate to severe hyperplastic change in the 14th and 20th week. The chemopreventive potential was determined by calculating the attributable risk (AR), which was –11.3 for the 14th week and increased up to –17.5 for the 20th week. To ascertain the effect of TMX treatment on inflammation, the effect of TMX on inflammatory cytokines was studied by ELISA. It revealed a significant reduction in inflammation upon TMX treatment for the 20th week. As TMX could hold its chemopreventive potential up to the 20th week, the molecular mechanism of restriction was studied for the 20th week of treatment. Skin forms a rich source of stem cells which orchestrate the progression of carcinogenesis and become cancer stem cells (CSCs). β-Catenin and KRAS are known central modulators of CSCs, that play a crucial role in the progression of skin carcinogenesis. We observed that TMX treatment inhibited KRAS and nuclear translocation of β-catenin causing its cytoplasmic degradation by P-53 and P-21-mediated pathway, thereby exerting its chemopreventive potential.

Keywords: Attributable risk, carcinogenesis, chemopreventive efficiency, mice, *Swertia chirata*, xanthone.

AMONG the various models of chemical carcinogenesis, mouse skin is popular for the study of cellular and biochemical changes such as proliferation characterized by hyper proliferation, and culminating into full-blown carcinogenesis bearing the potential for invasion and metastasis[1,2]. One of the triggering events during initiation of carcinogenesis is the mutation to R as proto-oncogenes giving the cells selective growth advantage. Deregulation of the Wnt signalling pathway plays a deciding role in the modulation of multistage carcinogenesis. Deregulation of the Wnt ligands enables cytoplasmic degradation of β-catenin by forming a destruction complex, which is made up of adenomatous polyposis coli (APC), scaffold protein axin, casein kinase 1 (CK1) and glycogen synthase kinase 3β (GSK3β)[3]. Interaction of Wnt ligands with the receptor complex that comprises Frizzled/LRP5/LRP6 (low-density lipoprotein receptor-related protein), causes modulation of a series of downstream events, leading to its stabilization and ultimately nuclear translocation of β-catenin[4]. Nuclear translocation of β-catenin modulates transcriptional regulation of multiple downstream oncogenic target genes involved in several process related to carcinogenesis[5]. Mutations in APC and KRAS have been proven to play a crucial role in carcinogenesis and induction of metastasis through enrichment of cancer stem cell (CSC) population[6]. GSK-3β causes proteasomal degradation of KRAS and β-catenin by polyubiquitination[7]. We already know that upregulation of β-catenin causes upregulation of several inflammatory markers[8]. Therefore, a molecule that could downregulate both β-catenin and KRAS is the need of the hour. As KRAS activation is considered to be one of the initiating events in skin cancer[9] and skin being one of the sites where β-catenin-mediated self-renewal plays a crucial role in the maintenance of its property to self-renew, we have chosen the 9,10-dimethylbenz[a]-anthracene (DMBA)/croton oil-mediated skin carcinogenesis model to evaluate the effect and elucidate the mechanism of 1,5,8-trihydroxy-3-methoxy xanthone (TMX) as a chemopreventive agent. Among the xanthones from *Swertia chirata*, TMX was the most active, as it showed therapeutic activity at the lowest dosage of 20 μg/kg (ref. 10). Therefore, in this study, we examine the effect exerted by TMX on DMBA-mediated skin carcinogenesis and

*For correspondence. (e-mail: prosenjit_cnci@yahoo.co.in)

also analyse the molecular mechanism of chemoprevention, if any.

Materials

DMBA and croton oil and secondary antibodies were procured from Sigma Aldrich, St Louis, USA. Primary antibodies were procured from Santa Cruz Biotechnologies. RNA isolation, cDNA synthesis and real-time PCR kits were procured from Roche Diagnostics Pvt Ltd., Risch-Rotkreuz, Switzerland rest of the chemicals were procured locally and were of molecular biology-grade.

Isolation and purification of TMX from S. chirata

Extraction, purification and characterization of TMX were performed at the Department of Biochemistry, National Research Institute for Ayurvedic Drug Development, Kolkata, India. The process of isolation is patented vide Indian Patent No. 191129, dated 26 March 2002 (refs 11–13).

Animals for experimentation

Adult (5–6 weeks old) Swiss mice (25 ± 2 g body wt) were obtained from the animal house of Chittaranjan National Cancer Institute, Kolkata. They were kept at astringently regulated environment with temperature of 23° ± 2°C and humidity 55% ± 10% under strictly maintained alternating light and dark conditions of 12 h each. Animals were provided with a standard food pellet diet and filtered drinking water according to the CPCSEA guidelines. All experimental procedures were carried out strictly following the protocols adhering to CPCSEA guidelines, which were approved by the Institutional Animal Ethics Committee (IAEC; approval no. IAEC-1774/PS-1/2015/8).

Development of skin carcinogenesis by DMBA

The dorsal part of the skin of Swiss mice was shaved with an electric razor three days before starting of the experiment, as adopted from a previously established model in our department[14]. The specific dose of carcinogen DMBA was 1 mg/100 µl of acetone/mouse and promoter 1% croton oil application, which was done topically on the area that had been shaved. Time point of gradual development of skin carcinoma was established by observing histopathological changes, where the number of animals sacrificed at each time point was two and experiments were repeated thrice. The body weight of mice was recorded every week since the beginning of the study and continued once weekly till the end-point, i.e. 20th week which was chosen following the humane guideline provided by the Organisation for Economic Co-operation and Development (OECD) as well as endorsed by CPCSEA and approved by IAEC. The appearance of papilloma(s) was documented every week during the study period with >1 mm in diameter considered as positive. Figure 1 *a* is a graphical representation of the treatment regime.

The animals were randomly divided into the following groups, where each group consisted of six animals and every experiment was repeated at least three times.

Normal control (NC): Neither carcinogen nor TMX was administered.

Carcinogen control (CC): Only carcinogen was administered as described in the graphical representation.

Continuous treatment (CT): TMX was administered two weeks prior to the first carcinogen administration and continued till the end-point of the study.

Cytoprotective effect of TMX against carcinogen-induced toxicity

In our study, blood was obtained by the method of cardiac puncture following the ethical guidelines from the animals of the experimental groups at the end of the experimental period of 20th week. The number of animals in each group were six, which was designated as $n = 6$. Serum was collected by separating from whole blood by following standard protocol of centrifugation at 2000 *g* for 15 min. Total blood parameters like counting of WBC, RBC, haemoglobin (HGB) and platelet (PLT) were measured from whole blood in an automated hematology analyzer (KX-21, Sysmex) following the manufacturer's protocol.

Cytoprotective efficacy of TMX against carcinogen-induced toxicity was evaluated by analysis of liver and kidney toxicity parameters of mice from the experimental group at the end of the 20th week. Hepato- and nephrotoxicity parameters like the expression of ALT, AST, urea and creatinine were analysed using an automated analyser for clinical samples (AU400, Olympus, Tokyo, Japan) following the manufacturer's guidelines (Olympus, Tokyo, Japan).

Phase-II antioxidative enzymes upon TMX treatment

Liver and skin samples were collected and lysates were prepared from liver and skin tissue obtained after sacrificing mice of the experimental group at the end of the experimental period, i.e. at the end of the 20th week. In the present study, the activity of phase-II detoxification enzymes like glutathione peroxidase (GPx), catalase (CAT), superoxide dismutase (SOD) and glutathione-S-transferase (GST) was measured in the skin and liver tissues of the mice from experimental groups of NC, CC and CT following previously described methods[15–17].

Intracellular ROS generation

Liver and skin lysates were prepared from liver and skin tissue obtained after sacrificing mice of the experimental

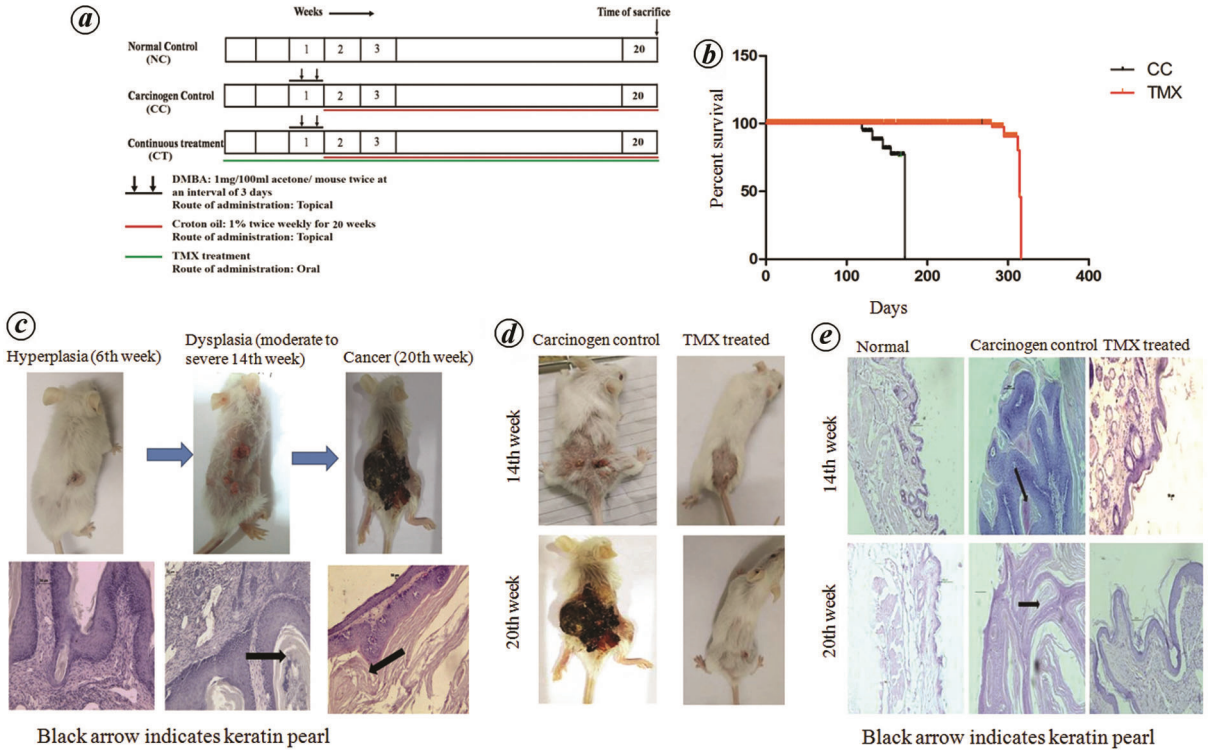

Figure 1. ***a***, Graphical representation of treatment regime of DMBA-induced mouse skin carcinogenesis model. ***b***, Graphical representation of Kaplan Maier survivability analysis in CC and CT experimental group. CT group showed significantly enhanced survival in comparison to CC group. Data represented as mean ± SD with significance $P < 0.0001$. ***c***, Developmental stages of skin carcinogenesis by DMBA-croton oil, hyperplasia, dysplasia and carcinoma *in situ*. The lower panel of histopathological gradation shows distinct stages of gradual progression to carcinogenesis. Black arrow indicates keratinization. Photographs were taken under 20× magnification using a bright-field microscope. ***d***, Macroscopic view of mice showing significant restriction of papilloma formation. ***e***, Representative photographs of histological evaluation of skin tissue of the experimental mice groups NC, CC and CT at the end of the 14th and 20th weeks. Blue arrow indicates atypia while black arrow indicates keratin pearl. Photographs were taken under 20× magnification using a bright-field microscope.

group at the end of the 20th week. The relative level of reactive oxygen species (ROS) of skin and liver lysate was analysed by spectrofluorimetric method as described by Pal *et al.*[14].

Modulation of membrane peroxidation upon TMX treatment

Hepatocytes and skin tissue were collected by sacrificing mice of the experimental group at the end of the experimental period (20th week). Lipid peroxidation (LPO) was estimated from the microsomal fraction extracted from hepatocytes and skin tissue lysates using thiobarbituric acid, and protein concentration was determined by a conventional method[19]. The representation was done by estimating the amount of thiobarbituric acid reactive substance (TBARS) formed per milligram protein using an extinction coefficient of $1.56 \times 10^5\ M^{-1}\ cm^{-1}$.

Effect of TMX on inflammation and angiogenesis

In the present study, the expression level of angiogenic and inflammatory markers was ascertained by ELISA. Blood was drawn from experimental mice by cardiac puncture and skin papillomas were collected after sacrifice of mice following ethical guidelines at the end of the 20th week. Serum was isolated from whole blood by a previously described method. Skin papillomas were made into single-cell suspension by finely mincing them in phosphate buffer saline and thereafter treatment with collagenase. Next, the samples were repeatedly passed through a syringe and a nylon mesh[20].

The level of different pro- and anti-inflammatory markers such as IL-10, IL-1β, IL-6, IL-18 and angiogenic markers such as VEGF, MMP-2, MMP-9 was measured in blood serum and skin papilloma lysates by ELISA method (Jiangsu Keygen Biotech Corp Ltd), following the manufacturer's protocol[21].

Histopathological analysis of papilloma

Three mice from each experimental group of NC, CC and CT were sacrificed according to the design of the experiment at two time points, i.e. 14th and 20th week. All the collected papilloma samples for each time point were fixed in 10% formaldehyde. Paraffin block for each papilloma

Table 1. Modulation of hematological and biochemical parameters upon TMX treatment of ascites-bearing mice

	Hematological parameters			
Group	White blood cell (/µl) × 10^3	Red blood cell (/µl) × 10^6	Haemoglobin (HGB; g/dl)	Platelets (/µl) × 10^3
Normal	15.6 (± 0.4)	4.69 (± 0.7)	8.7 (± 0.4)	319 (± 5)
Carcinogen control	87.8 (± 0.5)	2.12 (± 0.8)	2.4 (± 0.8)	879 (± 11)
TMX-treated	17.2 (± 0.2)**	5.05(± 0.5)**	10 (± 2)**	341 (± 8)**

	Biochemical parameters				
Group	Alkaline phosphate (IU/litre)	Aspartate transaminase (AST/SGOT) (IU/litre)	Alanine transminases (ALT/SGPT) (IU/litre)	Urea (mg/dl)	Creatinine (mg/dl)
Normal	47.8 (± 0.2)	219 (± 5)	69 (± 3)	52 (± 1)	0.7 (± 0.01)
Carcinogen control	197.5 (± 0.5)	879 (± 3)	315 (± 2)	133 (± 2)	1.5 (± 0.09)
TMX-treated	52.8 (± 0.7)*	211 (± 6)*	72 (± 2)*	51 (± 0.9)*	0.6 (± 0.02)*

*Significant difference in the TMX-treated group in comparison with carcinogen control group considering $P < 0.001$. Values represent ± SEM of six samples in each group. IU, International unit.

sample was prepared following a standardized protocol of our laboratory. From each paraffin block, 4 µm-thick sections of pappilloma were made using a microtome (Leica RM40, Wetzlar, Germany) and after complete deparaffinization with xylene followed by rehydration with a down-gradation of alcohol, were stained with hematoxylin and eosin (H&E)[22]. The slides were examined under different magnifications (10×, 20×, 40×) using a bright-field microscope and the observations were validated by a pathologist.

Role of TMX on cellular apoptosis

This study validated apoptosis by TUNEL assay (Roche Molecular Biochemicals, Manheim, Germany) according to the manufacturer's protocol. Data were acquired by visualizing the tissue sections under a bright-field microscope (Leica).

Protein expression analysis

In this study, immunohistochemistry (IHC) was performed on skin tissue following a protocol established in our laboratory with slight modifications of the method described by Prince and Ginsberg[23]. The protein expression pattern was scored according to Perrone *et al.*[24].

For immunoblot, total protein from skin tissue samples was extracted by sonication in RIPA buffer under chilled condition. The total protein lysate was resoluted by SDS-PAGE. The immunoreactive protein bands on the membranes were visualized using chemiluminescence reagents (Millipore, Germany) in chemi-doc gel documentation (Biorad, USA)[25].

mRNA expression analysis of different genes

RNA was isolated from skin tissue using Roche high-pure RNA isolation kit according to the manufacturer's guidelines. cDNA synthesis and real-time analysis were performed using cDNA synthesis kit and FastStart Essential DNA Green Master (Roche Life Science, Risch-Rotkreuz, Switzerland) respectively, according to the manufacturer's protocol[26].

Nuclear cytoplasmic fractionation

Subcellular fractionation from fresh tissue was based on the protocol described by Baghirova *et al.*[27]. After fractionation, it was cross-checked by Western blotting with the corresponding loading control GAPDH for cytoplasmic and lamin for nuclear loading control.

Detection of serum β-catenin

Serum β-catenin was detected by ELISA using mouse β-catenin (β-cat) ELISA kit (CSB-E11307m; Cusabio) following the manufacturer's protocol.

Statistical analysis

To find out whether TMX treatment had any significant effect, the *t*-test was performed between carcinogen control group and TMX treatment group, where $P < 0.05$, $P < 0.005$ and $P < 0.0001$ were considered as statistically significant. Data were represented as mean with standard deviation (SD) of at least three different experiments.

Results

Modulation of biochemical and hematological parameters

The haematological and biochemical parameters tell us whether TMX treatment could impart chemo-protection to the mice whose health detoriated due to the malignant

Table 2. Detoxifying enzymes, endogenous LPO and reactive oxygen species (ROS) level in liver and skin tissue

Group	GSH (nmol/mg)	GST (nmol/mg)	Gpx (nmol/mg)	SOD (unit/mg)	CAT (unit/mg)	LPO (moles/mg)	ROS (relative level)
Sample: Liver							
NC	3 (± 0.4)	5 (± 1)	5 (± 0.9)	9 (± 2)	3.9 (± 0.6)	3.5 (± 1.6)	1
CC	0.75 (± 0.6)	2.15 (± 0.86)	3.5 (± 0.7)	6.39 (± 1.8)	1.4 (± 0.1)	12 (± 1.2)	6
CT	4.72 (± 1)*	12 (± 1)*	7.9 (± 0.9)*	23 (± 1) #	4.7 (± 0.8)*	4 (± 0.7)*	2.1*
Sample: Skin							
NC	2 (± 0.6)	3 (± 1)	6 (± 2)	11 (± 3)	4.9 (± 0.39)	2.5 (± 0.6)	1
CC	0.89 (± 0.8)	1.75 (± 0.8)	3.8 (± 0.9)	5 (± 1)	2.4 (± 0.4)	11 (± 2)	7
CT	4.97 (± 0.7)*	6.15 (± 0.3)*	8.9 (± 0.3)*	14 (± 2)*	5.7 (± 0.5)*	4 (± 3)*	2*

*Significant difference in the CT group is found from the CC group considering $P < 0.0001$. Values represent ± SEM of six samples in each group.

condition induced by skin carcinogenesis. Increased levels of WBC and PLT count was normalized when TMX was administered at the non-toxic dosage to the carcinogen-treated mice. RBC and HGB levels were also modulated in a way that it became comparable to normal (Table 1). A similar trend of TMX-mediated normalization of elevated biochemical parameters was observed ($P < 0.001$) in comparison with carcinogen control (Table 1).

Survivability of mice after treatment with TMX

Survivability of mice on being treated with TMX was significantly increased in comparison to carcinogen control (Figure 1 *b*). An increase in the survivability of carcinogen-exposed mice is an indication of the therapeutic efficacy of this natural compound.

Phase-II detoxifying enzymes, LPO and ROS

It was observed that carcinogen exposure caused augmentation of endogenous LPO and ROS levels in the mouse skin and liver, whereas in the TMX-treated sample an abatement of these two parameters was observed (Table 2). Similarly, antioxidative enzymes which were suppressed due to carcinogenic exposure increased in a significant manner ($P < 0.0001$) following TMX treatment in the same set of samples.

Development of skin carcinogenesis by DMBA and croton oil

The gradual progression of skin carcinogenesis was initiated with the appearance of papilloma(s) after the sixth week of the first carcinogen application. To study the progression of carcinogenesis, we collected papillomas from two animals at different time points and the experiment was repeated thrice. The histology was analysed by H&E staining and confirmed by an expert pathologist. Our analysis revealed that there was a mild to moderate hyperplasia around the sixth week by the thickening of the epithelial layer. Progression to the dysplastic stage (severe) was noted around the 14th week. The disordered cellular stratification and increased nuclear: protoplasm (n/p) ratio exhibited the characteristic signature of the dysplastic stage. Thereafter, the progression to well-differentiated carcinoma *in situ* around the 20th week was characterized by well-developed keratinization with distinct pearl body and moderate atypia (Figure 1 *c*).

Evaluation of restrictive potential of TMX

The incidence of papilloma, i.e. tumour growing exophytically from the dorsal area, was observed around the 6th week after the first application of the carcinogen, whereas the time of incidence was significantly delayed, around the 14th week in the treated mice. Table 3 provides data on the incidence and inhibition of multiplicity of papillomas in the experimental groups at the 14th and 20th week, when well-differentiated carcinoma was observed in the CC group. It was also observed that the incidence of papilloma in the group which received TMX treatment was reduced by 50% with 79% inhibition of multiplicity at the end of 14th week and 55.5% with 80.8% inhibition of multiplicity at the end of 20th week in the CC group. Histological evaluation of the papillomas of the experimental group showed thickening of epidermal lining along with the formation of keratin pearl body and abnormally shaped cells called atypia in the CC group, which started around the 14th week and progressed into well-differentiated carcinoma around the 20th week is the prominent feature of invasion. In the treated samples, formation of pearl body was absent and a significantly lesser percentage of atypia was seen for both time points. There was thickening of the epidermal lining but overall architecture was close to normal, indicating suppression of invasive property of carcinogen after TMX treatment (Figure 1 *d* and *e*).

Effect of TMX on inflammatory and angiogenic markers

It was found from a previous analysis that TMX confers protective potential to mice during the progression of

Table 3. Incidence of papilloma and inhibition of multiplicity

Groups (n = 18)	No. of papilloma bearing mice	Incidence of papilloma (%)	No. of papilloma/ papilloma-bearing mice	Inhibition of multiplicity (%)
NC	00	(–)	(–)	(–)
CC (14th week)	15	83.3	4.3 (± 0.3)	0
CC (20th week)	18	100	6.8 (± 0.83)	0
CT (14th week)	9	50	0. 9 (± 0.01)	79
CT (20th week)	10	55.5	1.3 (± 0.82)	80.8

Inhibition of multiplicity: $\frac{(\text{Total no. of papilloma in CC} - \text{Total no. of papilloma in treated})}{\text{Total no. of papilloma in CC}} \times 100.$

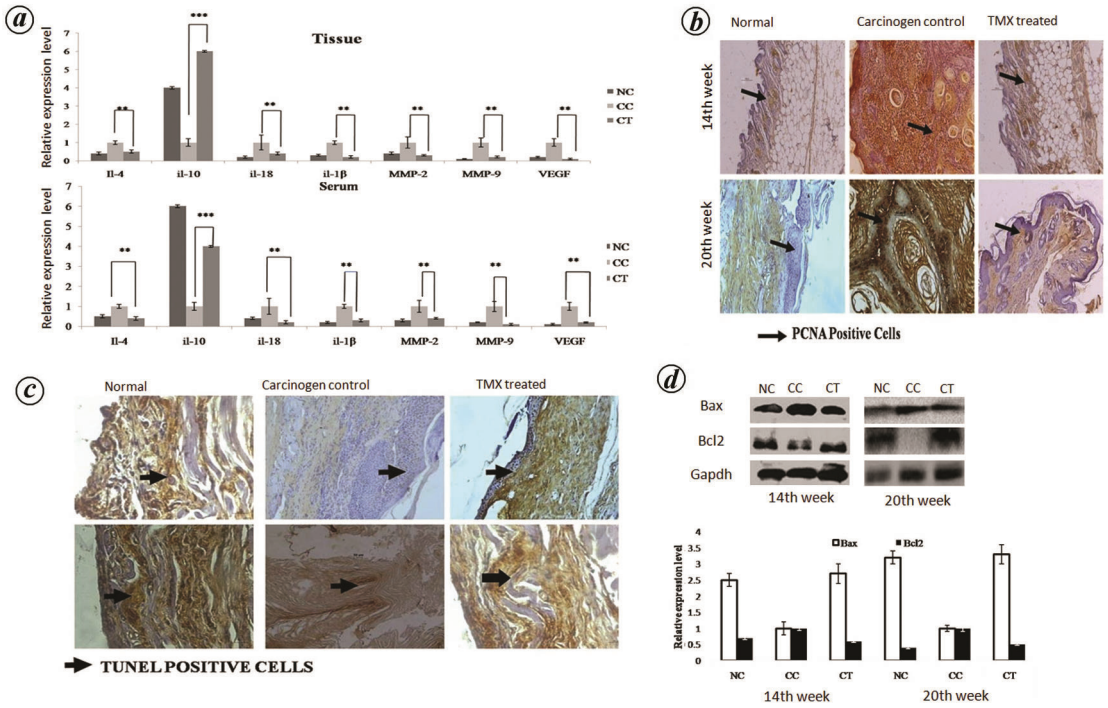

Figure 2. ***a***, Diagramatic representation of the relative expression levels of the pro- and anti-inflammatory and angiogenic markers as observed by ELISA. Tissue and serum from the mice of experimental groups NC, CC and CT show upregulation of anti-inflammatory factor IL-10, whereas all pro-inflammatory and angiogenic factor levels are reduced significantly. Data are represented as mean ± SD with significance $P < 0.05$. ***b***, Representation of PCNA expression levels by immune-histochemical staining. Representative photomicrographs of PCNA-positive cells are indicated by arrows. The photographs were taken under 20× magnification using a bright-field microscope. Percentage of proliferative cells is shown in NC, CC and CT experimental groups. Significantly reduced PCNA expression is observed in CT compared to CC for both 14th and 20th weeks. Data are represented as mean ± SD with significance $P < 0.0001$. ***c***, Representation of *in situ* TUNEL assay (apoptotic population) in skin-tissue samples of the experimental groups. Representative microscopic photomicrographs of TUNEL-positive cells are indicated by arrows. Photographs were taken under 20× magnification using a bright-field microscope. Increased cell death is found in CT group incomparison to CC group. A graphical representation shows the percentage of apoptotic population in the experimental groups NC, CC and CT for both 14th and 20th weeks. Data are represented as mean ± SD with significance $P < 0.0001$. ***d***, Expression of BAX and BCL-2 by Western blot of the experimental groups NC, CC and CT for both 14th and 20th weeks. Representative blots show reduced BCL-2 expression and increased BAX expression in CT group incomparison to CC group for both time points. Densitometric analysis through graphical representation shows the relative expression of individual markers. Peak density is normalized by the loading control GAPDH. Data are represented as mean ± SD with significance $P < 0.0001$.

DMBA/croton oil-induced skin carcinogenesis. The underlying factors that impact their role in providing protection are the pro- and anti-inflammatory markers along with the angiogenic markers. In the present study, we found that TMX treatment of carcinogen-exposed mice resulted in significant downregulation of pro-inflammatory factors and angiogenic markers like IL-4, IL-1β, IL-6 and IL-18, VEGF, MMP-2 and MMP-9, and upregulation of anti-inflammatory factors like IL-10 ($P < 0.05$) in comparison to the CC group (Figure 2 *a*). Therefore, these factors reinforce the preventive efficacy of TMX during the progression of induced carcinogenesis.

Role of TMX on cellular proliferation

Evaluation of the effect of TMX on the proliferation of skin tissue was analysed by IHC of this proliferation marker. The percentage of proliferative cells (dark-brown

Table 4. Effect of TMX on the relative risk due to cell proliferation and relative protection from apoptosis during skin carcinogenesis

Group	Incidence of proliferative cells (%; ± SEM)	Relative risk factor (RRF)	Incidence of apoptotic cells (%; ± SEM)	Relative protective factor (RPF)
Normal	12 ± 0.7	–	27 ± 0.6	–
Carcinogen control (14th week)	80.24 ± 0.4	6.66	19.47 ± 2	0.7
TMX-treated (14th week)	20.21 ± 2	1.68**	50.49 ± 5	1.87**
Carcinogen control (20th week)	90.5 ± 3	7.5	12 ± 1	0.4
TMX-treated (20th week)	22.1 ± 2	1.83**	61.5 ± 2	2.22**

***P*-value is <0.005. RRF, Incidence of proliferative cells after carcinogenic exposure/incidence of proliferative cells without carcinogenic exposure. RPF, Incidence of apoptotic cells after carcinogenic exposure/incidence of apoptotic cells without carcinogenic exposure.

Table 5. Incidence and frequency of papilloma in mouse skin at 14th and 20th week following exposure to DMBA/croton oil and treated with TMX correlated with an attributable risk

Parameters	Carcinogen control (14th week)	TMX-treated (14th week)	Carcinogen control (20th week)	TMX-treated (20th week)
RRF	6.66	1.68**	7.5	1.83
RPF	0.7	1.87**	0.4	2.22
Attributable risk (AR; %)	89.4	–11.3**	94.6	–17.5**
Incidence of papilloma (IP; %)	95	32	96	35
Multiplicity of papilloma (MP)	4.8 ± 0.2	1.8 ± 1	4.9 ± 0.1	1.9 ± 2

***P*-value is <0.005. AR = ((RRF – RPF)/RRF) × 100. IP = ((Incidence of papilloma in CC – incidence of papilloma in treated)/(Incidence of papilloma in CC)) × 100. MP = ((No. of papilloma/mouse in CC – no. of papilloma/mouse in treated)/(No. of papilloma/mouse in CC)) × 100.

nucleated cells) was determined from the total number of nuclei at ten randomly chosen microscopic fields of skin lesion. A significant ($P < 0.0001$) reduction in the expression of proliferating cell nuclear antigen (PCNA) was observed for the CT group compared to the carcinogen control group for both the 14th and 20th weeks of treatment (Figure 2 *b*).

Induction of apoptosis in skin tissue

The framework of drug-induced cell death helps reinforce the mechanism by which the malignancy burden is reduced. The percentage of apoptotic cells (dark-brown nucleated cells) was determined from the total number of nuclei counted at ten randomly chosen microscopic fields of skin lesion. A significant increase ($P < 0.0001$) in the percentage of apoptotic cells was found by TUNEL assay in the epithelial region in the CT group of samples in contrast to the CC group. Therefore, carcinogenesis is restricted in the skin tissue by restricting cell proliferation and induction of apoptosis for both the 14th and 20th weeks of TMX treatment (Figure 2 *c*).

Mechanisms of induction of apoptosis

Increased BAX/BCL-2 ratio is a well-known marker of the intrinsic pathway of apoptosis[28]. Therefore, to examine whether TMX could induce apoptosis by an intrinsic pathway, here the effect of TMX on BAX/BCL-2 was examined. A significant increase in the ratio in CT for both the 14th and 20th weeks was observed in comparison to CC, and it was comparable to NC where $P < 0.0001$ (Figure 2 *d*).

Risk assessment

The relative risk factor (RRF) in the carcinogen control group at 14 and 20 weeks due to cell proliferation was 6.66 and 7.5 respectively, whereas in groups receiving TMX treatment it was significantly lower (1.68 and 1.83 respectively). TMX treatment caused a significant increase in the relative protective factor (RPF) which was due to increased apoptosis. Similarly, there was a significant decrease in relative risk factor (RRF) upon TMX treatment which was due to decreased proliferation. In the carcinogen control group, the values of RPF were 0.7 and 0.4, which were significantly increased as a result of TMX treatment to 1.87 and 2.22 for the two time points studied respectively (Tables 4 and 5). The attributable risk (AR) can be calculated on account of the incidence of papilloma produced upon exposure to DMBA and croton oil with or without any type of intervention. It was noted that AR in CC after the 14th and 20th weeks was 89.4% and 94.6% respectively. This had reduced to –11.3% and –17.5% respectively, after TMX treatment (Tables 4 and 5), which is indicative of the chemopreventive effect of the xanthone.

Role of TMX on modulation of cancer stem cell markers

CSCs are a small subpopulation of tumour cells with capabilities of self-renewal, differentiation, tumorigenicity

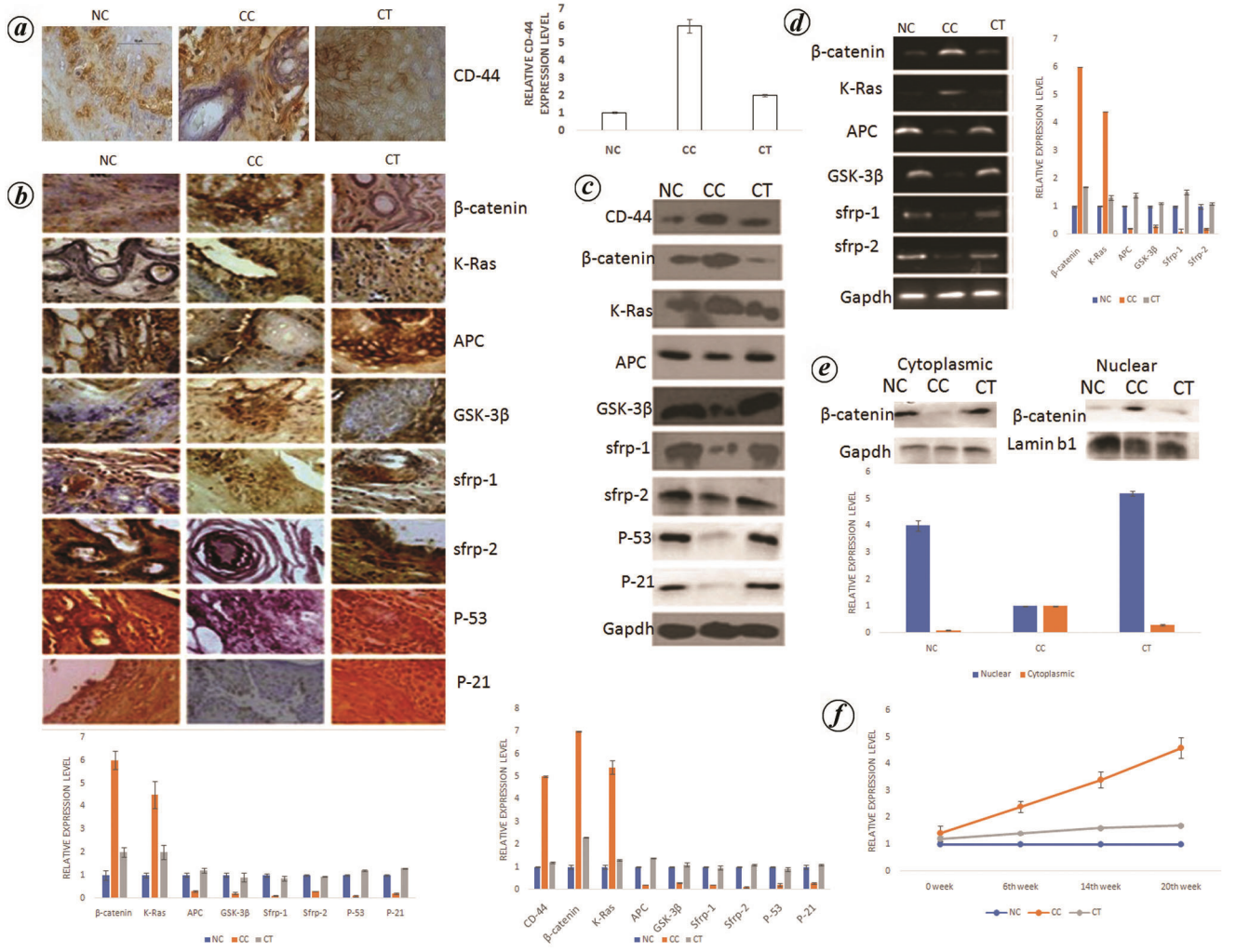

Figure 3. ***a***, Representation of CD44 expression by immunohistochemistry (IHC). In the skin carcinogenesis model, significant downregulation of CD-44 expression is observed. Photographs were taken under 20× magnification using a bright-field and fluorescence microscope. ***b***, Representation of *β*-catenin, K-RAS, P-53, APC, GSk-3*β*, SFrp1/2 expression by IHC. Significant modulation is observed with all the genes showing expressions comparable to the normal upon TMX treatment. Photographs were taken under 20× magnification using a bright-field and fluorescence microscope. ***c***, Expression of CSC markers and associated markers of CSC self-renewal pathway in all the models in respective experimental groups. Relative peak density is normalized with loading control GAPDH. ***d***, Relative mRNA expression of *β*-catenin and other markers of the Wnt/*β*-catenin pathway by quantitative RT-PCR. Downregulation of *β*-catenin and KRAS expression is observed in the treated group. In contrast, upregulation of APC, GSk-3*β* and SFrp1/2 is observed. ***e***, Nuclear cytoplasmic fractionation showing downregulation of nuclear translocation of *β*-catenin upon TMX treatment. Relative peak density of nuclear fraction is normalized by loading control lamin b1 and relative peak density of cytoplasmic fraction is normalized with GAPDH. ***f***, Serum level of *β*-catenin is seen to increase gradually with the progress of carcinogenesis, which is significantly restricted upon treatment with TMX.

when transplanted into a host[29] and are the prime reason for drug resistance and metastasis. The cell-surface marker CD44 is often used to identify the CSC subset with aggressive characteristics like proliferation, migration, angiogenesis, etc. It is reported that a regulatory network between the Wnt/*β*-catenin pathway and CD44 controls the CSC properties in cancer[30]. It has been suggested that the initial activation of Wnt/*β*-catenin signalling by APC loss is further enhanced by the stabilization of the oncogenic K-RAS protein[31]. Therefore, for a more detailed study on the molecular mechanism, we evaluated whether TMX could modulate the CSC population. Our data as validated by both IHC and Western blot analysis delineated that expression of CD44, B-catenin and KRAS is significantly reduced, while APC, GSK-3B Sfrp1/2, P-53, and P21 are significantly upregulated in the treated condition in comparison with the CC group (Figure 3 *a–c*).

Role of TMX on mRNA

The change in the transcriptional level reinforced that alteration in expression was undoubtedly owing to modulation in the mRNA level. TMX treatment significantly upregulated markers APC, GSK3*β*, which are the regulators of *β*-catenin, along with the other two important regulators, SFRP1 and SFRP2. Conversely significant

downregulation of β-catenin and KRAS was also observed $P < 0.0001$ (Figure 3 *d*).

Role of TMX on β-catenin

In the CC group, we observed highly upregulated nuclear β-catenin whereas significantly downregulated cytoplasmic β-catenin. Interestingly, upon TMX treatment, there was a significant increase in the cytoplasmic fraction of β-catenin and a decrease in the nuclear fraction as degradation of β-catenin occurs in the cytoplasm, thereby downregulating the transcription of several downstream oncogenes participating in carcinogenesis (Figure 3 *e*).

Correlation with carcinogenesis progression and serum β-catenin

Serum-level β-catenin was observed to increase sequentially with the progression of carcinogenesis in the 0th, 6th, 14th and 20th weeks in the CC group. TMX treatment showed an almost comparable level of serum β-catenin to NC at each time point up to the 20th week (Figure 3 *f*).

Discussion and conclusion

Polyphenols exhibit antioxidant activity by two main pathways, either by scavenging radicals to circumvent the cellular damage by ROS or by acting as molecules which can avert ROS production[32]. Antioxidants counteract oxidative stress, either enzymatically (vitamin C or E, or β-carotene) or non-enzymatically (superoxide dismutase), catalase or glutathione peroxidase to protect the cell organelles. Several epidemiological studies have demonstrated that changes in lifestyle and dietary habits could prevent or reduce cancer incidence[33]. In this study, we observed that TMX imparts cytoprotection against stress imparted by carcinogen treatment by upregulating phase-II detoxifying enzymes, and improving hematological and biochemical parameters. Increased levels of Wnt/β-catenin due to carcinogenic changes lead to overexpression of inflammatory cytokines like IL-4, IL-6, IL-1β and IL-18. Other molecules whose upregulation has been linked to increased levels of β-catenin are VEGF, MMP-2 and MMP-9, as these are known to be a downstream transcriptional target of β-catenin. Therefore, β-catenin is one of the central regulators in carcinogenesis[4,34]. Our data show that TMX treatment significantly downregulates inflammatory cytokines IL-4, IL-6, IL-1β and IL-18, and angiogenic markers MMP-2, MMP-9 and VEGF. Apoptosis plays an important role in chemotherapeutic and chemopreventive potential. There are many naturally occurring chemopreventive agents whose mode of action is the induction of apoptosis in cancer cells[35]. The cell proliferation and apoptosis balance is a crucial factor for carcinogenesis[36]. AR was calculated by counting the number of proliferative and non-proliferative cells at the target site, i.e. skin lesion, with and without exposure to a carcinogen (normal), modifying the method described by Burnekreef[37]. A 0% AR indicates that the risk generated due to exposure to a carcinogen is completely nullified by the compound under study, or there is no risk. Values greater than 0, signify some risk depending on the extent. A negative value qualifies the compound to have cancer-preventive potential. In this study we observed that TMX could efficiently induce apoptosis and reduce AR% to –11.3 and –17.5 after treatment for 14th and 20th weeks in the skin carcinogenesis model, which is indicative of its chemopreventive potential. P-53 plays a key role in the regulation of apoptosis. P-53 is one of the major targets of the Wnt signalling pathway, where cytoplasmic degradation of β-catenin has a central role[38]. P-53 induces activation of SIAH-1 (E3 ubiquitin ligase), which causes ubiquitination of β-catenin enabling its degradation. P53-mediated degradation of β-catenin simultaneous with cell-cycle arrest may play a central role in chemoprevention[39]. Glycogen synthase kinase-3β (GSK3β) has a vital role in the Wnt signalling pathway. P-53 activation is induced by DNA damage, which in turn transactivates GSK-3β. This activation is driven by direct binding of P-53 and GSK-3β, and causes the translocation of the latter to the nucleus. GSK-3β transactivation by P-53 promotes responses to the latter, including an increase in the P-21 levels[40]. Almost 30% of metastatic tumours have activating mutations in KRAS and 70% of metastatic tumours have loss-of-function mutations in TP-53 (ref. 41). Similar results are observed in the present study in the CC group when compared to the NC group. β-Catenin is an important component in the cell membrane and plays a role in cell adhesion. Upon receiving carcinogenic stimulus cells direct the nuclear translocation of β-catenin and various factors to carry forward the process of carcinogenesis[42]. TMX treatment significantly decreases the serum level of β-catenin, which was found to be significantly upregulated in the CC group. TMX treatment also significantly downregulated the total β-catenin, KRAS and nuclear translocation of β-catenin, with a significant upregulation of APC, GSK-3b Sfrp1/2, P-53 and P-21.

In conclusion, this study establishes that TMX has a chemopreventive potential and it does so by mediating cytoplasmic degradation of β-catenin by P-53- and P-21-mediated pathways.

1. Hennings, H. *et al.*, Critical aspects of initiation, promotion, and progression in multistage epidermal carcinogenesis. *Proc. Soc. Exp. Biol. Med.*, 1993, **202**, 1–8.
2. Slaga, T. J., Budunova, I. V., Gimenez-Conti, I. B. and Aldaz, C. M., The mouse skin carcinogenesis model. *J. Invest. Dermatol. Symp. Proc.*, 1996, **1**, 151–156.
3. Behrens, J. *et al.*, Functional interaction of an axin homolog, conductin, with beta-catenin, APC, and GSK3beta. *Science*, 1998, **280**, 596–599.

4. Huang, H. and He, X., Wnt/β-catenin signaling: new (and old) players and new insights. *Curr. Opin. Cell Biol.*, 2008, **20**, 119–125.
5. Mosimann, C., Hausmann, G. and Basler, K., Beta-catenin hits chromatin: regulation of Wnt target gene activation. *Nature Rev. Mol. Cell Biol.*, 2009, **10**, 276–286.
6. Lee, S.-K., Hwang, J.-H. and Choi, K.-Y., Interaction of the Wnt/β-catenin and RAS-ERK pathways involving co-stabilization of both β-catenin and RAS plays important roles in the colorectal tumorigenesis. *Adv. Biol. Regul.*, 2018, **68**, 46–54.
7. Shin, W. *et al.*, Identification of Ras-degrading small molecules that inhibit the transformation of colorectal cancer cells independent of β-catenin signaling. *Exp. Mol. Med.*, 2018, **50**, 1–10.
8. Lin, J. C. *et al.*, β-Catenin overexpression causes an increase in inflammatory cytokines and NF-κB activation in cardiomyocytes. *Cell. Mol. Biol.*, 2016, **63**, 17–22.
9. Caulin, C. *et al.*, An inducible mouse model for skin cancer reveals distinct roles for gain- and loss-of-function *p53* mutations. *J. Clin. Invest*, 2007, **117**, 1893–1901.
10. Barua, A., Choudhury, P., Mandal, S., Panda, C. K. and Saha, P., Therapeutic potential of xanthones from *Swertia chirata* in breast cancer cells. *Indian J. Med. Res.*, 2020, **152**, 285–295.
11. Barua, A., Choudhury, P., Mandal, S., Panda, C. K. and Saha, P., Anti-metastatic potential of a novel xanthone sourced by *Swertia chirata* against *in vivo* and *in vitro* breast adenocarcinoma frameworks. *Asian Pac. J. Cancer Prev.*, 2020, **21**, 2865–2875.
12. Barua, A., Panda, C. and Saha, P., Chemotherapeutic potential of novel xathone sourced from *Swertia chirata* against skin carcinogenesis. *Asian J. Pharm. Clin. Res*., 2020, **13**, 84–88.
13. Barua, A., Choudhury, P., Maity, J. K., Mandal, S. B., Mandal, S. and Saha, P., Chemotherapeutic potential of novel non-toxic nucleoside analogues on EAC ascetic tumour cells. *Free Radic. Res.*, 2019, **53**, 57–67.
14. Pal, D., Banerjee, S., Mukherjee, S., Roy, A., Panda, C. K. and Das, S., Eugenol restricts DMBA croton oil induced skin carcinogenesis in mice: downregulation of *c*-Myc and H-ras, and activation of p53 dependent apoptotic pathway. *J. Dermatol. Sci.*, 2010, **59**, 31–39.
15. Habig, W. H., Pabst, M. J. and Jakoby, W. B., Glutathione S-transferases. The first enzymatic step in mercapturic acid formation. *J. Biol. Chem.*, 1974, **249**, 7130–7139.
16. Johansson, L. H. and Borg, L. A., A spectrophotometric method for determination of catalase activity in small tissue samples. *Anal. Biochem.*, 1988, **174**, 331–336.
17. Paglia, D. E. and Valentine, W. N., Studies on the quantitative and qualitative characterization of erythrocyte glutathione peroxidase. *J. Lab. Clin. Med.*, 1967, **70**, 158–169.
18. Yamamoto, T. *et al.*, Roles of catalase and hydrogen peroxide in green tea polyphenol-induced chemopreventive effects. *J. Pharmacol. Exp. Ther.*, 2004, **308**, 317–323.
19. Ohkawa, H., Ohishi, N. and Yagi, K., Assay for lipid peroxides in animal tissues by thiobarbituric acid reaction. *Anal. Biochem.*, 1979, **95**, 351–358.
20. Heidari-Soreshjani, S., Asadi-Samani, M., Yang, Q. and Saeedi-Boroujeni, A., Phytotherapy of nephrotoxicity-induced by cancer drugs: an updated review. *J. Nephropathol.*, 2017, **6**, 254–263.
21. Sporn, M. B., Approaches to prevention of epithelial cancer during the preneoplastic period. *Cancer Res.*, 1976, **36**, 2699–2702.
22. Wu, C. F., Double-staining in toto with hematoxylin and eosin. *Science*, 1940, **92**, 515–516.
23. Prince, A. M. and Ginsberg, H. S., Immunohistochemical studies on the interaction between Ehrlich ascites tumor cells and Newcastle disease virus. *J. Exp. Med.*, 1957, **105**, 177–188.
24. Perrone, F. *et al.*, Molecular and cytogenetic subgroups of oropharyngeal squamous cell carcinoma. *Clin. Cancer Res.*, 2006, **12**, 6643–6651.
25. Burnette, W. N., 'Western blotting': electrophoretic transfer of proteins from sodium dodecyl sulfate–polyacrylamide gels to unmodified nitrocellulose and radiographic detection with antibody and radioiodinated protein A. *Anal. Biochem.*, 1981, **112**, 195–203.
26. Schneeberger, C., Speiser, P., Kury, F. and Zeillinger, R., Quantitative detection of reverse transcriptase-PCR products by means of a novel and sensitive DNA stain. *PCR Methods Appl.*, 1995, **4**, 234–238.
27. Baghirova, S., Hughes, B. G., Hendzel, M. J. and Schulz, R., Sequential fractionation and isolation of subcellular proteins from tissue or cultured cells. *MethodsX*, 2015, **2**, 440–445.
28. Hata, A. N., Engelman, J. A. and Faber, A. C., The BCL-2 family: key mediators of the apoptotic response to targeted anti-cancer therapeutics. *Cancer Discov.*, 2015, **5**, 475–487.
29. Yu, Z., Pestell, T. G., Lisanti, M. P. and Pestell, R. G., Cancer stem cells. *Int. J. Biochem. Cell Biol.*, 2012, **44**, 2144–2151.
30. Cheng, Y. *et al*., Physiological β-catenin signaling controls self-renewal networks and generation of stem-like cells from nasopharyngeal carcinoma. *BMC Cell Biol.*, 2013, **14**, 44.
31. Moon, B.-S., Jeong, W.-J., Park, J., Kim, T. I., Min, D. S. and Choi, K.-Y., Role of oncogenic K-Ras in cancer stem cell activation by aberrant Wnt/β-catenin signaling. *J. Natl. Cancer Inst.*, 2014, **106**, 373–383.
32. Perron, N. R. and Brumaghim, J. L., A review of the antioxidant mechanisms of polyphenol compounds related to iron binding. *Cell Biochem. Biophys.*, 2009, **53**, 75–100.
33. Anand, P. *et al*., Cancer is a preventable disease that requires major lifestyle changes. *Pharm. Res.*, 2008, **25**, 2097–2116.
34. Aumiller, V., Balsara, N., Wilhelm, J., Günther, A. and Königshoff, M., WNT/β-catenin signaling induces IL-1β expression by alveolar epithelial cells in pulmonary fibrosis. *Am. J. Res. Cell Mol. Biol.*, 2013, **49**, 96–104.
35. Taraphdar, A. K., Roy, M. and Bhattacharya, R. K., Natural products as inducers of apoptosis: implication for cancer therapy and prevention. *Curr. Sci.*, 2001, **80**, 1387–1396.
36. Bedi, A. *et al.*, Inhibition of apoptosis during development of colorectal cancer. *Cancer Res.*, 1995, **55**, 1811–1816.
37. Brunekreef, B., Environmental epidemiology and risk assessment. *Toxicol. Lett.*, 2008, **180**, 118–122.
38. Gross, A., McDonnell, J. M. and Korsmeyer, S. J., BCL-2 family members and the mitochondria in apoptosis. *Genes Dev.*, 1999, **13**, 1899–1911.
39. Matsuzawa, S. I. and Reed, J. C., Siah-1, SIP and Ebi collaborate in a novel pathway for beta-catenin degradation linked to p53 responses. *Mol. Cell*, 2001, **7**, 915–926.
40. Abbas, T. and Dutta, A., p21 in cancer: intricate networks and multiple activities. *Nature Rev. Cancer*, 2009, **9**, 400–414.
41. Murata, J., Saiki, I., Matsuno, K., Tokura, S. and Azuma, I., Inhibition of tumor cell arrest in lungs by antimetastatic chitin heparinoid. *Jpn. J. Cancer Res.*, 1990, **81**, 506–513.
42. Hatsell, S., Rowlands, T., Hiremath, M. and Cowin, P., Beta-catenin and Tcfs in mammary development and cancer. *J. Mamm. Gland Biol. Neoplasia*, 2003, **8**, 145–158.

Received 3 July 2021; revised accepted 22 November 2021

doi: 10.18520/cs/v122/i4/429-438